A Real-Time Potential Flow–CFD Coupling Method for Floating Bodies with Heave Plates

Wei Meng[1], Yiren Li[1], Zhuang Kang[1,2*] and Gong Chen[1]

[1]MIIT Key Laboratory of Deep-Sea Engineering Equipment and Technology,
College of Shipbuilding Engineering, Harbin Engineering University,
No. 145 Nantong Street, Nangang District, Harbin, Heilongjiang, China

[2]Taihu Laboratory of Deepsea Technological Science,
No. 266 Shanshui East Road, Binhu District, Wuxi, Jiangsu, China

*E-mail: kangzhuang@hrbeu.edu.cn

1 INTRODUCTION

Heave plates are widely utilized on floating offshore structures to suppress wave-induced motions. This motion reduction is achieved through two primary mechanisms, including viscous damping generated by flow separation and vortex shedding around the plate edges, and an increase in added mass, which shifts the natural heave period away from predominant wave periods.

High-fidelity Computational Fluid Dynamics (CFD) methods provide detailed insights into vortex dynamics, but the associated computational cost is prohibitive for long-duration simulations or extensive parametric studies [1]. A common approach is to augment potential-flow solvers with Morison-type drag terms [2], though these empirical corrections often require case-specific tuning [3]. Moreover, added-mass and damping coefficients exhibit strong dependence on the Keulegan–Carpenter (KC) number [4]. Recent advances introduce KC-adaptive algorithms [5] that incorporate amplitude- and frequency-dependent C_d coefficients, thereby reducing reliance on empirical calibration. However, these approaches can still incur significant computational costs in terms of acquiring the C_d data sets and exhibit limited adaptability to varied geometries, while also suffering from phase inaccuracies in time-domain response predictions.

This study introduces a real-time coupling method that integrates a potential-flow solver with a locally refined single-phase CFD solver. Implemented in *OpenFOAM*, the coupling solver is validated against published experimental data and two-phase CFD simulations for heave-plated cylinders, encompassing single- and dual-plate spar spar configurations in free decay and forced oscillation. Compared to the two-phase CFD method, the proposed approach delivers substantial computational savings while effectively capturing the essential viscous phenomena that govern KC-dependent hydrodynamic response.

2 NUMERICAL METHODS

The present real-time coupling solver consists of a potential-flow solver based on the impulse response function method [6] and a single-phase CFD solver for the incompressible Navier–Stokes equations. The two solvers employ the same equations of motion, with forces from both contributing to update the body motions.

The equation of motion for a heaving floating body is

$$(M + A_{33}^{\infty} - A_{33}^{0})a_3 = -\int_0^t K_{33}(t-\tau)v(\tau)d\tau + F^{HST}(t) + F^{CFD}(t), \tag{1}$$

where M is the mass of the floating body, A_{33}^{∞} is the added mass at infinite frequency, A_{33}^{0} is the added mass at zero frequency, a_3 is the acceleration in the heave direction, F^{HST} and F^{CFD} are the hydrostatic restoring forces and CFD forces, respectively, and K_{33} is the retardation function computed as

$$K_{33}(\tau) = \frac{2}{\pi}\int_0^{\infty} B_{33}(\omega)\cos\omega\tau\, d\omega. \tag{2}$$

where B_{33} is the damping coefficient. It should be noted that the term $A_{33}^{0}a_3$ is included to cancel the low-frequency added mass contribution that is accounted for in F^{CFD}.

The governing equations of the CFD solver are

$$\nabla \cdot \mathbf{u} = 0, \tag{3}$$

$$\frac{\partial \mathbf{u}}{\partial t} + \nabla \cdot [\mathbf{u}(\mathbf{u} - \mathbf{u}_m)] = -\nabla p + \nabla \cdot (\nu_{\text{eff}} \nabla \mathbf{u}), \tag{4}$$

where $\mathbf{u}$ and $\mathbf{u}_m$ are the fluid and mesh velocities, respectively, p denotes the pressure, and ν_{eff} represents the effective kinematic viscosity.

Turbulence is modeled using the k–ω SST model, and mesh motion is handled via Laplacian morphing. At each time step, the potential-flow and CFD solvers exchange motion information to update forces, and the equations of motion are integrated using a two-step Adams–Bashforth scheme. This hybrid framework captures essential viscous effects while providing substantial computational savings compared to fully viscous simulations.

3 RESULTS AND DISCUSSION

A series of cylindrical spar models with identical diameter and draft are selected to validate the present coupling solver through free-decay tests. Following the configuration adopted by Rao et al.[7], the diameter of cylinder, D_c, is set to 0.15 m, the draft, d, to 0.385 m, and the diameter of heave plate, D_p, to 0.15 m. As shown in Fig. 1(a), two configurations are considered, including a single-plate spar model and dual-plate spar models with plate spacings, S, of 0.20 m, 0.10 m, and 0.05 m, respectively. The plate thickness is 0.003 m.

The free-decay responses obtained from the present coupling solver are compared with experimental measurements from the literature [7], as well as with results from a two-phase CFD solver based on *OpenFOAM*. The time histories of the displacement are presented in Fig. 1(b)–(e). Overall, good agreement is observed between the present results and the reference data, confirming the validity of the proposed coupling method. In terms of computational cost, the mesh used in the present coupling solver consists of 0.5 M cells, with local refinement around the heave plates. The two-phase CFD solver employs a mesh of 4.2 M cells, refined both near the free surface and around the heave plates. The corresponding computational times are 0.6 h using 16 cores and 11 h using 48 cores, respectively. Note that all simulations were conducted on AMD EPYC 7532 CPUs.

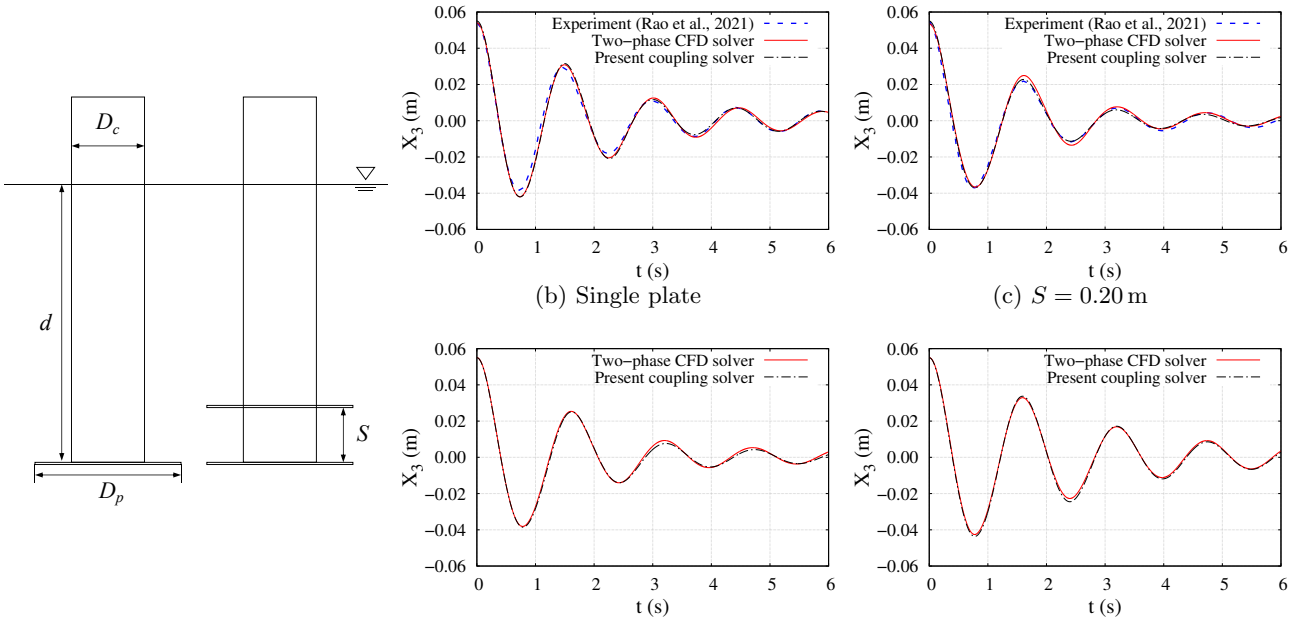

(a) Spar models (b) Single plate (c) $S = 0.20$ m (d) $S = 0.10$ m (e) $S = 0.05$ m

Figure 1: Schematic diagram of spar configurations and comparison of free-decay test results.

Furthermore, damping ratios and natural periods of the single-plate and dual-plate spar models are listed in Table 1. Consistent values are obtained from both the two-phase CFD solver and the present coupling solver. It can be observed that the damping ratio of the dual-plate model with a small plate spacing (S=0.05 m) is lower than that of the single-plate model. As the plate spacing increases, the damping ratio increases accordingly; however, once the spacing reaches a certain threshold, the damping ratio exhibits only slight variations.

To further investigate the flow mechanisms associated with varying plate spacings, vortex structures around the dual-plate spar models are visualized at selected instants within one oscillation period, as shown in Fig. 2. In each subfigure, the left side depicts the vortex structures obtained from the single-phase CFD solver, while the right side shows those from the two-phase solver. A strong similarity between the two results is observed. As can be inferred from the first ($S = 0.05$ m) and second rows ($S = 0.10$ m) of Fig. 2, the increase in damping with greater plate spacing can be attributed to a transition from suppressed vortex shedding at closer spacings,

Table 1: Comparison of damping ratios and natural periods

S	ζ [% discrepancy]		T_n (s) [% discrepancy]	
	Two-phase CFD solver	Present coupling solver	Two-phase CFD solver	Present coupling solver
-	0.1147	0.1209 [5.41]	1.4870	0.1506 [1.28]
0.05	0.0937	0.0927 [1.07]	1.5980	1.5950 [0.19]
0.10	0.1471	0.1549 [5.30]	1.6005	1.6120 [0.72]
0.20	0.1597	0.1734 [8.58]	1.6080	1.5960 [0.75]

where vortex interactions are suppressed, to more independent vortex development at larger spacings, allowing stronger vortex formation and enhanced energy dissipation.

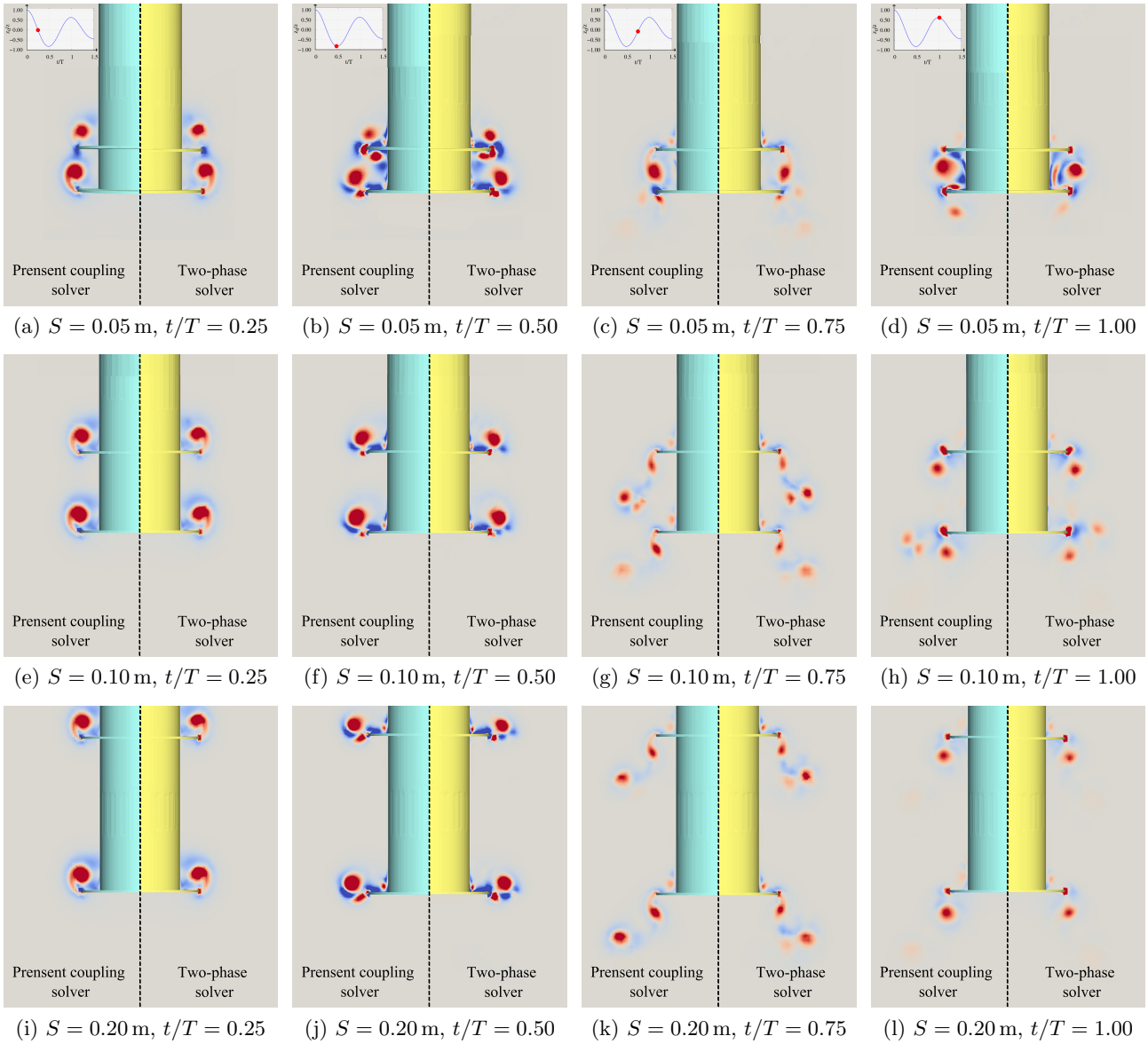

(a) $S = 0.05\,\text{m}$, $t/T = 0.25$ (b) $S = 0.05\,\text{m}$, $t/T = 0.50$ (c) $S = 0.05\,\text{m}$, $t/T = 0.75$ (d) $S = 0.05\,\text{m}$, $t/T = 1.00$

(e) $S = 0.10\,\text{m}$, $t/T = 0.25$ (f) $S = 0.10\,\text{m}$, $t/T = 0.50$ (g) $S = 0.10\,\text{m}$, $t/T = 0.75$ (h) $S = 0.10\,\text{m}$, $t/T = 1.00$

(i) $S = 0.20\,\text{m}$, $t/T = 0.25$ (j) $S = 0.20\,\text{m}$, $t/T = 0.50$ (k) $S = 0.20\,\text{m}$, $t/T = 0.75$ (l) $S = 0.20\,\text{m}$, $t/T = 1.00$

Figure 2: Vortex structures during free decay simulation

The present real-time coupling solver inherently separates the total hydrodynamic force acting on the floating body into radiation force and viscous force associated with flow separation. To further quantify the damping effect of the dual-plate models with different plate spacings, forced oscillations at an excitation frequency, ω, of 3.85 rad/s with an amplitude, A, of 0.03 m are conducted for the dual-plate spar models with $S = 0.05\,\text{m}$ and 0.20 m. Fig. 3 presents the time histories of the vertical radiation and viscous forces. It can be seen that the radiation force component remains nearly identical for the two configurations, even though the model with larger plate spacing generates stronger wave radiation. In contrast, viscous force contributes dominantly to the

total damping response and exhibits pronounced higher-order harmonic components. These results indicate that the differences in motion-suppression performance between the dual-plate spar models with $S = 0.05\,\mathrm{m}$ and $0.20\,\mathrm{m}$ are primarily governed by variations in viscous load.

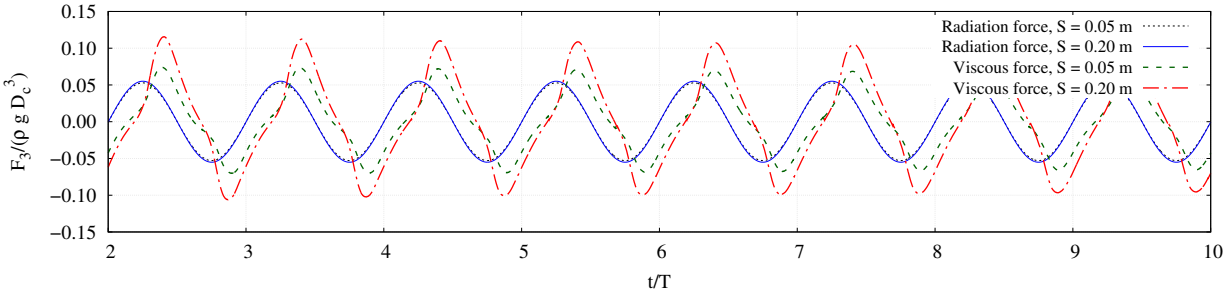

Figure 3: Radiation and viscous forces under forced oscillation

Referring to Fig. 2, at small spacing (first row, $S = 0.05\,\mathrm{m}$), vortex interference between the two plates tends to suppress coherent vortex shedding, thereby limiting flow separation and viscous dissipation. In contrast, at larger spacings (second and third rows, $S = 0.10\,\mathrm{m}$ and $0.20\,\mathrm{m}$), the flow allows the formation of two nearly independent vortex-shedding systems, resulting in superimposed unidirectional vortex shedding accompanied by intensified flow separation and increased viscous dissipation. Further increasing the spacing from $0.10\,\mathrm{m}$ to $0.20\,\mathrm{m}$ leads to only marginal variations in the hydrodynamic damping.

4 CONCLUSION

A real-time coupling method, combining a potential-flow solver with a single-phase CFD solver, has been developed to model the hydrodynamic response of heave-plated floating structures. The coupling solver produces free-decay responses for both single- and dual-plate spar models that align closely with experimental data and results from two-phase CFD simulations. Using this coupling approach, the hydrodynamic effects of plate spacing in dual-plate spars are investigated. The results show that increasing the plate spacing enhances viscous damping due to a transition from suppressed vortex shedding to independent vortex development. However, beyond a certain threshold spacing, further increases yield only marginal changes in the motion response. The present solver offers significant computational efficiency and enables the separation of different force components, providing insight into the hydrodynamic behavior of heave-plated floating bodies.

References

[1] S. An and O. M. Faltinsen, "An experimental and numerical study of heave added mass and damping of horizontally submerged and perforated rectangular plates," *Journal of Fluids and Structures*, vol. 39, pp. 87–101, 2013.

[2] J. Morison, J. Johnson, and S. Schaaf, "The force exerted by surface waves on piles," *Journal of Petroleum Technology*, vol. 2, pp. 149–154, 05 1950.

[3] L. Tao and D. Dray, "Hydrodynamic performance of solid and porous heave plates," *Ocean engineering*, vol. 35, no. 10, pp. 1006–1014, 2008.

[4] G. H. Keulegan and L. H. Carpenter, "Forces on cylinders and plates in an oscillating fluid," *Journal of research of the National Bureau of Standards*, vol. 60, no. 5, pp. 423–440, 1958.

[5] Y.-L. Shao, J. You, and E. B. Glomnes, "Stochastic linearization and its application in motion analysis of cylindrical floating structure with bilge boxes," *International Conference on Offshore Mechanics and Arctic Engineering*, vol. 1, p. V001T01A016, 06 2016.

[6] S. J. Liapis, *Time-domain Analysis of Ship Motions*. PhD thesis, University of Michigan, 1986.

[7] M. J. Rao, S. Nallayarasu, and S. Bhattacharyya, "CFD approach to heave damping of spar with heave plates with experimental validation," *Applied Ocean Research*, vol. 108, p. 102517, 2021.